Routes to chaos in a model of a bursting neuron

C. C. Canavier, J. W. Clark, and J. H. Byrne*

Department of Electrical and Computer Engineering, Rice University, Houston, Texas 77251-1892; and *Department of Neurobiology and Anatomy, University of Texas Medical School, Houston, Texas 77225 USA

ABSTRACT   Chaotic regimes have been observed experimentally in neurons as well as in deterministic neuronal models. The R15 bursting cell in the abdominal ganglion of *Aplysia* has been the subject of extensive mathematical modeling. Previously, the model of Plant and Kim has been shown to exhibit both bursting and beating modes of electrical activity. In this report, we demonstrate (*a*) that a chaotic regime exists between the bursting and beating modes of the model, and (*b*) that the model approaches chaos from both modes by a period doubling cascade. The bifurcation parameter employed is the external stimulus current. In addition to the period doubling observed in the model-generated trajectories, a period three "window" was observed, power spectra that demonstrate the approaches to chaos were generated, and the Lyaponov exponents and the fractal dimension of the chaotic attractors were calculated. Chaotic regimes have been observed in several similar models, which suggests that they are a general characteristic of cells that exhibit both bursting and beating modes.

INTRODUCTION

Chaos in neural systems can be operationally defined as activity which appears random but is generated by a deterministic system rather than by additive noise. Consequently, there is no need to invoke a random process to account for aperiodic, irregular behavior if the presence of a chaotic regime can be established. A chaotic system is one in which long-term prediction of the system's state is impossible because of the unavoidable finite uncertainty in determining the initial state (37, 40)

Once chaotic activity is suspected, several representations which serve to identify such activity are listed in order of increasing power to resolve periodic from aperiodic behavior: time domain records, phase plane trajectories, power spectra, and Poincaré return maps (9, 15, 32). The above methods are primarily useful to characterize the periodic regimes which frequently culminate in chaos via the well-known period doubling route to chaos (10, 11). The period doubling route to chaos can be characterized as follows. At a given value of a nonlinearity (bifurcation) parameter, a periodic regime with a fundamental period (1P) prevails; as the bifurcation parameter is adjusted, the period of the system doubles each time the system undergoes a bifurcation until the system has an infinite period which characterizes chaos. As the bifurcation parameter is adjusted further, "windows" with odd periods appear, such as a stable three cycle (3P). The odd periods then themselves undergo period doubling to chaos (9, 13). The three cycle has a

special significance because in a one-dimensional mapping its existence implies chaos (30).

Finally, the method that provides the definitive mathematical signature of a chaotic attractor is its spectrum of Lyaponov exponents (14, 41). In quantitative terms, an attractor is chaotic if it has one or more positive Lyaponov exponents (14). The number of Lyaponov exponents associated with a given system is equivalent to the number of its state variables. A positive exponent is associated with divergence, a zero exponent with a limit cycle, and a negative exponent with convergence (41).

Chaotic regimes have been observed experimentally in neurons (16–18, 24) as well as in deterministic neuronal models (3, 5). To investigate possible chaotic regimes in individual neurons, we examined a mathematical model of a widely studied invertebrate neuron. Cell R15 of the marine mollusc *Aplysia* exhibits a normal endogenous bursting mode (2, 12) and a beating mode if either the sodium-potassium pump is pharmacologically blocked or a constant depolarizing current is injected into the cell (25). A mathematical model of R15 has been developed by Plant and Kim (36), which qualitatively mimics these modes of electrical activity. Bursting behavior in R15 is a result of the interaction of variables for membrane conductances on two time scales, one fast and the other slow (35). The action potentials or spikes result from the fast conductances whereas bursts result from the slow conductances. Thus, in the bursting mode the slow and fast

rhythms act as coupled oscillators and the slow oscillator dominates. In contrast, in the beating (nonbursting) mode the fast rhythms dominate. Given the basic features of the activity of R15, as well as the structure of the mathematical model for the behavior of this cell, it appeared to us that it could in principle exhibit chaotic behavior. Our simulations revealed that the model of R15 does indeed exhibit chaotic behavior, as a single bifurcation parameter (the external stimulus current) is varied while holding all other parameters constant.

METHODS

The Plant and Kim model represents a unit area of cell membrane and consists of a membrane capacitance in parallel with a number of ionic conductances. The ionic conductances consist of two Na^+ conductances (g_{Na} and g_T), a delayed rectifier K^+ conductance (g_K), a transient outward K^+ conductance (g_A), a slowly varying potassium conductance ($g_{K,s}$), and a leakage conductance (g_L). Additional parallel elements are a sodium-potassium pump current (I_{EP}) and an external stimulus current (I_{STIM}). This equivalent circuit is similar to the Hodgkin-Huxley (H-H) model (22) of the squid giant axon but has been expanded to include: (a) a constant sodium conductance (g_T) representing the tetrodotoxin-insensitive inward current (36), (b) a transient outward K^+ conductance (g_A) with an activation variable r and an inactivation variable s, (c) a slowly varying ($\tau = 8$ s) potassium conductance ($g_{K,s}$) which has an activation variable q and can be equated with the Ca^{2+}-dependent potassium conductance (35), and (d) a sodium-potassium pump represented by a constant hyperpolarizing current (I_{EP}). The equation for membrane potential is derived from Kirchoff's Current Law:

$$\dot{V} = -(I_{Na} + I_K + I_A + I_{K,s} + I_L - I_{EP} - I_{STIM})/C_m. \quad (1)$$

The gating variables are described by first order differential equations of the following form, for m, h, n, q, r, and s:

$$\dot{x} = (x_\infty - x)/\tau_x, \quad (2)$$

where x represents the particular variable and τ its time constant. Note that Plant and Kim scaled and translated the voltage term in the equations for the alpha and beta rate constants for the H-H gating variables m, h, and n. The following apparent typographical errors in the original paper [36] were rectified by inserting the following: (a) a factor of 1.2 scaling the voltage term in the denominator of the expression for α_m, (b) a pair of brackets enclosing the argument of the exponential in the expression for α_h, and (c) a minus sign preceeding the constant part of the argument of the exponential in the expressions for α_m, β_m, and β_h. Thus, the corrected expressions used in this study are:

$$\alpha_m = 0.1(-26 - 1.2V)/exp\,[(-26 - 1.2V)/10] - 1 \quad (3)$$

$$\beta_m = 4\,exp\,[(-51 - 1.21V)/18] \quad (4)$$

$$\alpha_h = 0.07\,exp\,[(-51 - 1.21V)/20\,] \quad (5)$$

$$\beta_h = 1/\{exp\,[(-21 - 1.3V)/10] + 1\}. \quad (6)$$

Otherwise, the parameters and equations are the same as those in the original paper (36).

The equations associated with the model were numerically integrated using a fourth-order Runge-Kutta-Merson algorithm both on a VAX 11/750 and a Sequent Symmetry S27 multiprocessor system. A variable step size was implemented using a tolerance for error in the voltage waveform of 0.001 mV. The minimum step size required was 0.5 ms. A discrepancy was noted in that for zero stimulus current, the original study (36) obtained seven spikes per burst, whereas the current study obtained four. This discrepancy may be a result of integration schemes or a result of the way in which the published model equations were corrected to compensate for apparent typographical errors. We used the temporal waveform of the gating variable q to generate the power spectra shown in Fig. 2. This variable was chosen because it is the most slowly-varying state variable and therefore dominates the rate of convergence (9). Although the variable q is unobservable, it may be interpreted as a dimensionless representation of the intracellular concentration of calcium, as the slowly-varying component of the potassium conductance is known to be calcium-dependent. The time course of q most clearly indicates the progression of period doubling. Samples of q were taken every 15.25 ms for 500 s which resulted in a 32768 point Discrete Fourier Transform (DFT). The Lyaponov exponents were calculated using the algorithm of Wolf et al. (41), employing Gram-Schmidt reorthonormalization every 100–250 ms for 300–3,000 s as required for convergence. Generally speaking, this algorithm is considered to have converged to within a few percent of its assymptotic values when the mandatory zero exponent is a few orders of magnitude smaller than the next smallest exponent (41). This algorithm required the integration of 56 simultaneous differential equations; the integration was implemented with the same Runge-Kutta-Merson method on the Sequent Symmetry multiprocessor system. The dimension of the attractors was estimated by the method of Kaplan and Yorke (27, 41).

RESULTS

The state space was explored as a single bifurcation parameter (I_{STIM}) was varied. A variety of modes was observed including two "back-to-back" period-doubling cascades (10, 11). What is known about the intricate structure of this well-known route to chaos as it applies to the results of our study can be summarized as follows. In this route period doublings are observed by a mechanism known as pitchfork bifurcations (32) until the system has an infinite period and exhibits chaotic behavior. These period doublings can easily be observed in a two-dimensional plane projection of the phase space as the limit cycle splits. The system then undergoes reverse bifurcations (33) as the attractor coalesces into "bands" of trajectories. In the terminology of Hao and Zhang (15), the original limit cycle is referred to as 1P and subsequent splittings are called 2P, 4P, and so on. The inverse bifurcation chaotic orbits are referred to as 1I, 2I, 4I and so on, depending on the number of chaotic bands The label "P" stands for periodic, and the label "I" stands for inverse (a term which is used interchangeably with reverse and denotes a chaotic orbit). The sequence of orbits 1P, 2P, 4P . . . 4I, 2I, 1I is referred to as a primary sequence. Interestingly, a secondary sequence of periodic regions and chaotic bands is embedded within each primary chaotic band. The periodic orbits arise by tangent bifurcations (32) (the type I intermittent route to

chaos). Each secondary orbit (either periodic or inverse within a primary kI band is always a multiple of k. The secondary orbits may be odd, thus in the primary 1I band it is possible to find 3P, 5P, 7P . . . regimes. Tertiary sequences have also been observed (15).

At a stimulus intensity of 0.22 μamps, the bifurcation parameter I_{STIM} exactly cancels the constant hyperpolarizing current by which the sodium-potassium pump is modeled. In this case, the model exhibits a beating behavior corresponding to an R15 neuron in which the sodium-potassium pump has been blocked pharmacologically. As I_{STIM} was decreased from a value corresponding to complete block of the sodium pump to one corresponding to normal operation the following regimes were observed: beating (0.2200–0.1885 μamps) (Figs. 1 and 2, A panels), a period-doubling sequence from a beating mode culminating in "chaotic beating" (0.1880–0.1865 μamps) (Figs. 1 and 2, panels B–D), a period-three window (0.18612 μamps) (Fig. 3) followed by period doubling to 6P (0.18605 μamps), again culminating in "chaotic beating" (0.1855 μamps) and a chaotic regime (0.184–0.128 μamps). Within this chaotic regime, the firing pattern evolves from a "chaotic beating" pattern to a pattern of "chaotic bursting". As I_{STIM} is decreased further, the behavior of the cell emerges from the "chaotic bursting" to 4P, 2P, and finally the normal 1P five-spike bursing mode (Fig. 4 A). This second period-doubling sequence occurs in the range from 0.128–0.110 μamps. Yet another "chaotic bursting" regime (0.18–0.068 μamps), a five-spike bursting region (0.065–0.025 μamps), and a four-spike bursing region (0.025–0.000 μamps) were also observed but are not shown here. Between the four- and five-spike regions there is a transition where both four- and five-spike bursts are generated.

Fig. 1 illustrates the beating 1P mode (A) and the transitions to the 2P mode (B), then the 4P mode (C), and finally "chaotic beating" (D) as a function of decreasing stimulus intensity. The time courses of the membrane voltage and the q gating variable, and the state space projection of the trajectories on the voltage vs. q plane are shown side by side for each parameter. The time course of the voltage does not indicate readily the period doubling, but it is quite clear in the waveform of the q gating variable. The period doubling appears in the phase plane plots as the splitting of the trajectories.

The results were also analyzed using power spectra and Poincaré return maps (Fig. 2). Discrete peaks appear at the fundamental frequency (0.22 Hz) and its harmonics (only the first one shown at 0.44 Hz) for the beating case (e.g., Fig. 2 A). In B the fundamental frequency is 0.2 Hz and the first subharmonic ($f_0/2$) appears at 0.1 Hz as a result of the period doubling. Two more subharmonic peaks appear at 0.05 and 0.15 Hz in C. This process
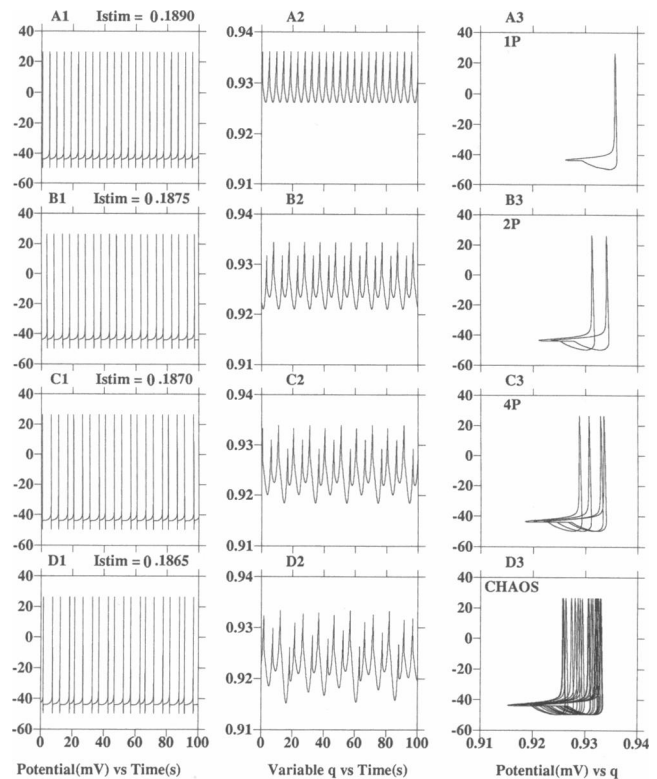

FIGURE 1 Time domain and phase plane representation of period-doubling cascade from the beating mode (A) as a function of decreasing I_{STIM} (B–D). In these and subsequent graphs, all transients were allowed to die out before any points were plotted.

continues until the spectrum appears noisy in the chaotic beating mode (D). Note that a discrete peak is still evident at the former fundamental frequency.

Poincaré return maps were constructed by sampling the values of the q gating variable at the peaks on the voltage waveform, then plotting the values of q vs. the previous value (Fig. 2, $A2$–$D2$). In other words, the Poincaré surface chosen is a line where potential equals approximately 26 mV (e.g., Fig. 1 $A3$). The system can be reduced to a single dimension due to the shrinkage of volumes in state space; that is, the direction of slowest convergence dominates, effectively reducing the system to one dimension (9). Evidence that this model is dominated by shrinkage in the direction associated with the gating variable q is provided by the fact that when one plots potential vs. a gating variable, phase plane splitting of trajectories is only observed in plots which include q, and by the consistent results obtained using the return maps constructed under the above assumption. The Poincaré return maps for the transition from the beating mode to chaos exhibit the classic shape which is quadratic about the maximum. After the transients have died out, the
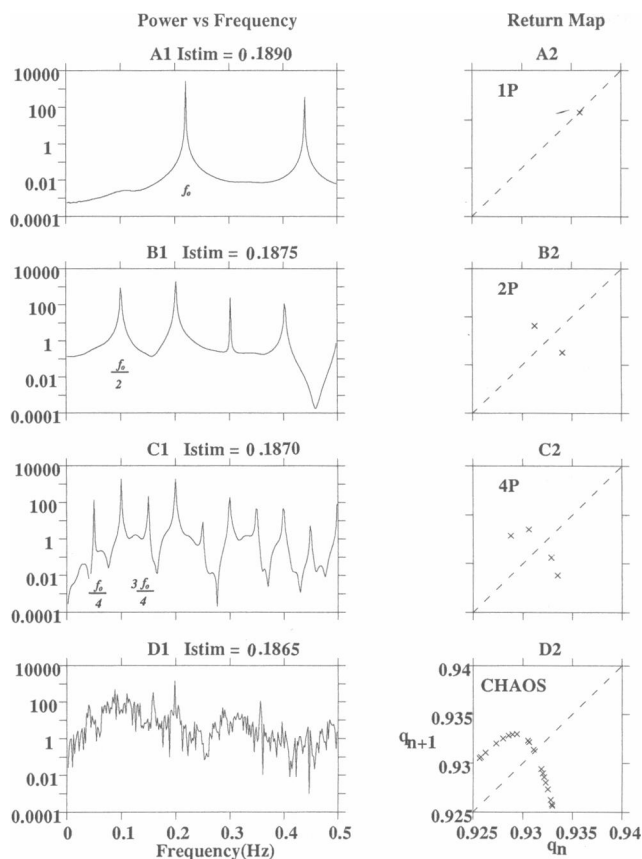
FIGURE 2 Power spectra and Poincaré return maps for period-doubling cascade from the beating mode as a function of decreasing I_{STIM}. A 32,768-point DFT was performed on the q waveform (e.g., panels $A2$, $B2$, $C2$, and $D2$ in Fig. 1). The results were then squared and plotted on semilogarithmic axes. f_o represents the fundamental frequency.

beating mode appears as a single point, the 2P mode as two points, and so on until the chaotic model fills the parabola with points.

The period-three window corresponds to triplets in the voltage waveform (Fig. 3). As the stimulus intensity is decreased yet further, "chaotic bursting" is observed as well as a second period doubling cascade from the oppo-
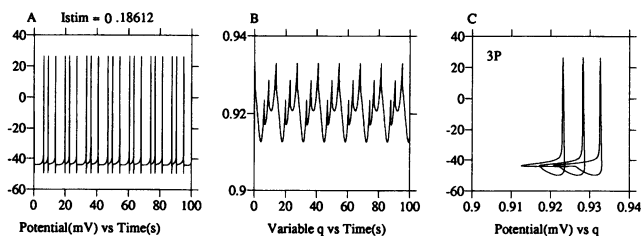

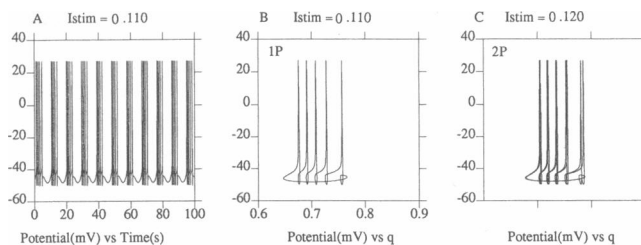FIGURE 3 Period-three window: time domain and phase plane representation.

FIGURE 4 Period doubling from the bursting mode: time domain and phase plane representation.

site direction. A typical bursting waveform (Fig. 4 A) corresponds to a 1P mode (B), whereas panel C demonstrates the splitting of the phase plane trajectories characteristics of the bifurcation to the 2P mode. The power spectra and Poincaré maps corresponding to the period-three window and the period-doubling cascade from the bursting mode into chaos are not shown, but the results were similar to those obtained in Fig. 2.

The results are summarized in a portion of a bifurcation tree (Fig. 5). This figure illustrates the progression from a periodic regime through chaos into another periodic regime. In general, a bifurcation tree is constructed by plotting the value of a state variable (in this case q) at
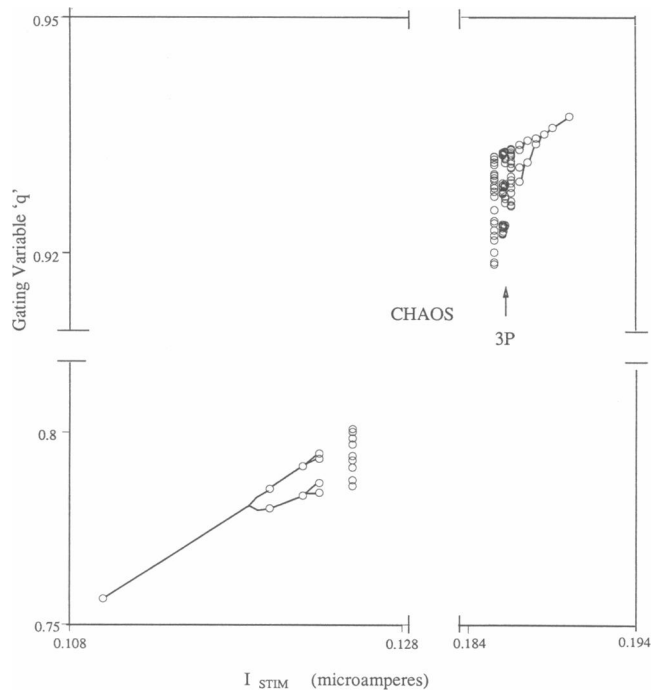

FIGURE 5 Bifurcation tree. Each branch indicates a period-doubling bifurcation. To show both approaches to chaos, two scales were required for both the ordinate and abscissa. The location of the period-three (3P) window in indicated as well as the large intermediate region of chaos.

all intersections with the Poincaré surface vs. the value of the bifurcation parameter (I_{STIM}). However, to construct the bifurcation tree of Fig. 5, only the points below the 45° line of the Poincaré return maps associated with the period doubling cascade from the bursting mode were used in order to have one point for the 1P mode, two points for the 2P mode, and so on. The spectrum of Lyaponov exponents in bits per millisecond for selected values of I_{STIM} is given in Table 1 along with the dimension of the attractor. Using the algorithm of Wolf et al. (41), the zero exponents converged to a value several orders of magnitude smaller than the next largest exponent for the values of I_{STIM} in the range 0.1855–0.1890 μamps; however, for the values 0.1100–0.1300 μamps, at convergence the zero exponent was only an order of magnitude smaller than the nearest exponent. Note that a fractal dimension was obtained for the chaotic attractors, whereas a limit cycle has a dimension of one.

DISCUSSION

Transitional chaotic regime

Our results indicate that the Plant and Kim model of R15 exhibits chaotic behavior. Thus, chaotic activity can be a result of intrinsic properties of individual neurons and need not be an emergent property of neural assemblies. The chaotic regime of the model is flanked by two period-doubling cascades, one from a bursting mode and one from a beating mode. A chaotic regime which was also approached from the same two modes by a period doubling cascade has been observed by Chay (5) in neuronal membrane model based on Eyring multibarrier rate theory. In addition, regions of chaotic behavior can be found in the Hindmarsh and Rose model (20), and in a three-variable model by Chay (6), as described by Kaas-Petersen (26). Finally, examples of chaotic beating and chaotic bursting have been observed in a model of a pancreatic beta cell (7). Based on our work and that of others, we infer that the transition from the beating to bursting mode frequently includes a chaotic regime and may in fact require one. In the intermediate region "the chaotic behavior appears as a compromise between two trends," as Hao and Zhang have commented regarding a

periodically-forced nonlinear oscillator (15). The detection of the period-three window, the power spectral evidence displayed in Fig. 2, and the Lyaponov exponents in Table 1 substantiate the existence of a chaotic regime more fully than in previous studies. (5, 7).

At the time the P-K model (36) and the neuronal model of Chay (4) were developed, the available experimental evidence indicated that the variation of internal calcium ion concentration modulated a calcium-activated K^+ conductance ($g_{K,Ca}$) and this variation in turn contributed casually to burst generation (25). Current evidence indicates however that $g_{K,Ca}$ is not the primary conductance that generates the bursting activity. Instead, calcium-dependent inactivation of the slow inward current appears to be critical (1, 28). Preliminary simulations including this additional mechanisms indicate that the basic conclusions presented here are unaltered (unpublished observations).

While the existence of chaotic behavior in R15 has not been examined experimentally in detail, our modeling results predict that the potential for such behavior exists. Indeed, because the bifurcation parameters employed in the model (I_{STIM}) are roughly equivalent to the current generated by the sodium-potassium pump, we predict that modulating the activity of this pump either physiologically or with appropriate doses of metabolic poisons would lead to chaotic regimes. Potentially chaotic firing patterns which are transitional between bursting and beating have been observed in Tritonia pacemaker neurons (39). Irregular bursting patterns and a transitional region between bursting and beating have also been observed in R15 in response to the application of 4-aminopyridine (4-AP) [19], which acts on potassium channels. Thus, the potassium conductances may also act as bifurcation parameters in some instances. Two other experiments further implicate the potassium conductances. First, molluscan neuron activity has been shown to bifurcate from a beating model to doublet spiking, to triplet spiking, and finally to a bursting mode (23) in response to iontopheretic injection of the K^+ channel blocker tetraethyl ammonium (TEA). Second, prolonged exposure to 4-AP has been shown to induce apparently chaotic discharges in molluscan neurons upon return to normal saline (24). Moreover, because the activity of

TABLE 1 Lyaponov exponents

I_{STIM}	λ_1	λ_2	λ_3	λ_4	λ_5	λ_6	λ_7	DIM
0.1890	0.0000	−0.0002	−0.0029	−0.0120	−0.0227	−0.0468	−0.1804	1.00
0.1865	0.0001	0.0000	−0.0026	−0.0123	−0.0224	−0.0479	−0.1757	2.04
0.1855	0.0001	0.0000	−0.0032	−0.0124	−0.0226	−0.0485	−0.1749	2.04
0.1300	0.0002	0.0000	−0.0053	−0.0149	−0.0300	−0.0665	−0.1626	2.04
0.1100	0.0000	−0.0003	−0.0044	−0.0145	−0.0305	−0.0711	−0.1569	1.00

R15, including the transition from the bursting to the beating mode, can be modulated by a variety of neurotransmitters (29, 31), such agents (at appropriate concentrations) may also lead to chaotic regimes, as could changes in the levels of internal and external calcium for the same reason.

Given the well-known intricate structure of the period-doubling route to chaos, the region of overlap between two "back-to-back" period-doubling cascades may be an interesting topic for mathematical investigation. The analysis in terms of a bifurcation tree is essentially one-dimensional and may not be adequate to describe this additional complexity fully in higher dimensional systems. This limitation does not apply to the multidimensional method of Lyaponov exponents employed in this study, however.

Significance of chaos

Although the number of reports of chaotic patterns in biological systems is growing, the physiological significance of chaos is poorly understood. It is clear, however, that chaos enables a deterministic system to generate variability which appears random but in fact does not rely on a random process. Variability is usually introduced into a system by noise, which obscures the signal. In a biological system generating a chaotic output, the variability may be the signal, or at least part of it. To illustrate the possibilities created by a chaotic regime, the generation of a behavior by a periodic signal can be contrasted with the generation of the same behavior by a chaotic one (8, 34). A behavior that is associated with a limit cycle can only be generated in a monotonous, repetitive fashion. Furthermore, a perturbation of the system requires that energy be dissipated to restore the limit cycle. On the other hand, a behavior associated with a chaotic attractor can be generated in an infinite number of ways. This variation may have adaptive advantages because disturbances are effectively dissipated in a chaotic system. For example, a small perturbation in the system will not prevent a normal output from being generated unless the perturbation is large enough to displace the trajectory out of the attractive basin of the chaotic attractor. This view is consistent with the suggestion that biological chaos prevents the various functional units from becoming entrained, or phase-locked, into periodic activity (8). Skarda and Freeman have suggested that the neurons in the olfactory system of rabbits exhibit chaotic dynamics in a background mode, that is, in the absence of a recognized order, and that upon recognition of a previously learned odor, the system bifurcates to a limit cycle attractor corresponding to that particular odor (21, 38). In their view, chaotic activity allows "rapid and unbiased access to every limit cycle attractor on every inhalation" (38), while still preventing cyclic entrainment or spatially structured activity.

REFERENCES

1. Adams, W. B., and I. B. Levitan. 1985. Voltage and ion dependences of the slow currents which mediate bursting in *Aplysia* neurone R15. *J. Physiol. (Lond.).* 360:69–93.

2. Alving, B.O. 1968. Spontaneous activity in isolated somata of *Aplysia* pacemaker neurons. *J. Gen. Physiol.* 51:29–45.

3. Carpenter, G. A. 1972. Bursting phenomena in excitable membranes. *SIAM J. Appl. Math.* 36:334–372.

4. Chay, T. R. 1983. Eyring rate theory in excitable membranes: application to neuronal oscillations. *J. Phys. Chem.* 87:2935–2940.

5. Chay, T. R. 1984. Abnormal discharges and chaos in a neuronal model system. *Biol. Cybern.* 50:301–311.

6. Chay, T. R. 1984. Chaos in a three-variable model of an excitable cell. *Physica.* 16D:233–242.

7. Chay, T. R. and J. Rinzel. 1985. Bursting, beating, and chaos in an excitable membrane model. *Biophys. J.* 47:357–366.

8. Conrad, M. 1986. What is the use of chaos? *In* Chaos. A. V. Holden, editor. Manchester University Press, Manchester, UK. 3–14.

9. Cvitanovic, P. 1984. Universality in chaos. *In* Universality in Chaos. P. Cvitanovic, editor. Adam Hilger Ltd., Bristol, UK. 3–34.

10. Feigenbaum, M. J. 1978. Quantitative universality for a class of nonlinear transformations. *J. Stat. Phys.* 19:25–52.

11. Feigenbaum, M. J. 1979. The universal metric properties of nonlinear transformations. *J. Stat. Phys.* 21:669–706.

12. Frazier, W. T., E. R. Kandel, I. Kupferman, R. Waziri, and R. Coggeshall. 1967. Morphological and functional properties of identified neurons in the abdominal ganglion of *Aplysia californica*. *J. Neurophysiol.* 30:1288–1351.

13. Gleick, J. 1987. Chaos. R. R. Donnelley and Sons, Harrisonburg, VA.

14. Grebogi, C., E. Ott, S. Pelikan, and J. A. Yorke. 1984. Strange attractors that are not chaotic. *Physica.* 13D:262–268.

15. Hao, B., and S. Zhang. 1982. Hierarchy of chaotic bands. *J. Stat. Phys.* 28:769–792.

16. Hayashi, H., M. Nakao, and K. Hirakawa. 1982. Chaos in the self-sustained oscillation of an excitable biological membrane under sinusoidal stimulation. *Phys. Lett.* 88A:265–266.

17. Hayashi, H., S. Ishizuka, and K. Hirakawa. 1983. Transition to chaos via intermittency in the *Onchidium* pacemaker neuron. *Phys. Lett.* 98A:474–476.

18. Hayashi, H., S. Ishizuka, M. Ohta, and K. Hirakawa. 1982. Chaotic behavior in the *Onchidium* giant neuron membrane under sinusoidal stimulation. *Phys. Lett.* 88A:435–438.

19. Hermann, A., and A. L. F. Gorman. 1981. Effects of 4-aminopyridine on potassium currents in a molluscan neuron. *J. Gen Physiol.* 78:63–86.

20. Hindmarsh, J. L., and R. M. Rose. 1984. A model of neuronal bursting using three coupled first order differential equations. *Proc. R. Soc. Lond.* B 221:87–102.

21. Hirsch, M. W. 1989. Convergent activation dynamics in continuous time networks. *Neural Networks.* 2:331–349.

22. Hodgkin, A. L., and A. F. Huxley. 1952. A quantitative description of membrane current and its application to conduction and excitation in nerve. *J. Physiol. (Lond.).* 117:500–554.

23. Holden, A. V., and W. Winlow. 1982. Bifurcation of periodic activity from periodic activity in a molluscan neuron. *Biol. Cybern.* 42:189–194.

24. Holden, A. V., W. Winlow, and P. G. Haydon. 1982. The induction of periodic and chaotic activity in a molluscan neuron. *Biol. Cybern.* 43:169–173.

25. Junge, D., and C. L. Stephens. 1973. Cyclic variation of potassium conductance in a burst-generating neurone in *Aplysia. J. Physiol. (Lond.).* 235:155–181.

26. Kaas-Petersen, C. 1987. Bifurcations in the Rose-Hindmarsh model and the Chay model. *In* Chaos in Biological Systems. H. Degn, A. V. Holden and L. F. Olsen, editors. Plenum Publishing Corp., New York. 183–190.

27. Kaplan, J. L., and J. A. Yorke. 1979. Chaotic behavior of multidimensional difference equations. *In* Functional Differential Equations and Approximation of Fixed Points. H. O. Peitgen and H. O. Walther, editors. Springer-Verlag, Berlin. 204.

28. Kramer, R. H., and Zucker. R. S. 1985. Ca^{2+} regulated currents in bursting neurones. *J. Physiol. (Lond.)* 362:131–160.

29. Levitan, E. S., and I. B. Levitan. 1988. A cyclic GMP analog decreases the currents underlying bursting activity in the *Aplysia* neruon R15. *J. Neurosci.* 8:1162–1171.

30. Li, T. Y. and J. A. Yorke. 1975. Period three implies chaos. *Am. Math. Monthly.* 82:985–992.

31. Lotshaw, D. P., and I. B. Levitan. 1988. Reciprocal modulation of calcium current by serotonin and dopamine in the identified *Aplysia* neuron R15. *Brain Res.* 439:64–76.

32. May, R. 1976. Simple mathematical models with very complicated dynamics. *Nature (Lond.)* 261:459–467.

33. Misiurewicz, M. 1981. Absolutely continuous measures for certain maps of an interval *Publ. Math. I.H.E.S.* 53:17.

34. Mpitsos, G. J., R. M. Burton, Jr., H. C. Creech, and S. O. Soinila. 1988. Evidence for chaos in spike trains of neurons that generate rhythmic motor patterns. *Brain Res. Bull.* 21:529–538.

35. Plant, R. E. 1981. Bifurcation and resonance in a model for bursting nerve cells. *J. Math Biol.* 11:15–32.

36. Plant, R. E., and M. Kim. 1976. Mathematical description of a bursting pacemaker neuron by a modification of the Hodgkin-Huxley equations. *Biophys. J.* 16:227–244.

37. Ruelle, D. 1984. Strange attractors. *In* Universality in Chaos. P. Cvitanovic, editor. Adam Hilger Ltd., Bristol, UK. 37–48.

38. Skarda, C. A., and W. J. Freeman. 1987. How brains make chaos in order to make sense of the world. *Behav. Brain Sci.* 10:161–195.

39. Smith, S. J., and S. H. Thompson. 1987. Slow membrane currents in bursting pace-maker neurones of *Tritonia. J. Physiol. (Lond.).* 382:425–448.

40. Wolf, A. 1986. Quantifying chaos with Lyapunov exponents. *In* Chaos. A. V. Holden, editor. Manchester University Press, Manchester, UK. 271–273.

41. Wolf, A., J. B. Swift, H. L. Swinney, and J. A. Vestano. 1985. Determining Lyaponov exponents from a time series. *Physica.* 16D:285–317.